FERMILAB-PUB-18-116-AE-PPD

YITP-SB-18-4, CERN-TH-2018-070

SENSEI: First Direct-Detection Constraints on sub-GeV Dark Matter from a Surface Run

The SENSEI Collaboration: Michael Crisler,[1,*] Rouven Essig,[2,†] Juan Estrada,[1,‡] Guillermo Fernandez,[1,§] Javier Tiffenberg,[1,¶] Miguel Sofo Haro,[1,3,**] Tomer Volansky,[4,5,††] and Tien-Tien Yu[6,7,‡‡]

[1] *Fermi National Accelerator Laboratory, PO Box 500, Batavia IL, 60510*
[2] *C.N. Yang Institute for Theoretical Physics, Stony Brook University, Stony Brook, NY 11794*
[3] *Centro Atómico Bariloche, CNEA/CONICET/IB, Bariloche, Argentina*
[4] *Raymond and Beverly Sackler School of Physics and Astronomy, Tel-Aviv University, Tel-Aviv 69978, Israel*
[5] *School of Natural Sciences, The Institute for Advanced Study, Princeton, NJ 08540, USA*
[6] *Theoretical Physics Department, CERN, CH-1211 Geneva 23, Switzerland*
[7] *Department of Physics and Institute of Theoretical Science, University of Oregon, Eugene, Oregon 97403*

The Sub-Electron-Noise Skipper CCD Experimental Instrument (SENSEI) uses the recently developed Skipper-CCD technology to search for electron recoils from the interaction of sub-GeV dark matter particles with electrons in silicon. We report first results from a prototype SENSEI detector, which collected 0.019 gram-days of commissioning data above ground at Fermi National Accelerator Laboratory. These commissioning data are sufficient to set new direct-detection constraints for dark matter particles with masses between ∼500 keV and 4 MeV. Moreover, since these data were taken on the surface, they disfavor previously allowed strongly interacting dark matter particles with masses between ∼500 keV and a few hundred MeV. We discuss the implications of these data for several dark matter candidates, including one model proposed to explain the anomalously large 21-cm signal observed by the EDGES Collaboration. SENSEI is the first experiment dedicated to the search for electron recoils from dark matter, and these results demonstrate the power of the Skipper-CCD technology for dark matter searches.

INTRODUCTION

Identifying the nature of dark matter (DM) is one of the most urgent tasks of particle physics today, and direct-detection experiments play an essential role in this endeavor. The search for DM particles with masses $\lesssim 1$ GeV represents a new experimental frontier [1]. Traditional direct-detection searches, which are sensitive to recoil energy generated from DM scattering off of nuclei, typically have very little sensitivity to sub-GeV mass DM. Indeed, the best current bounds are limited to very large cross sections below 1 GeV and are absent below ~ 120 MeV [2–4]. As suggested in [5], improved sensitivity to DM masses well below the GeV scale is possible by searching for signals induced by inelastic processes, for which a DM particle is able to deposit much more energy compared to the elastic scattering off of nuclei. In particular, one of the most promising avenues is to search for one or a few ionized electrons that are released due to DM particles interacting with electrons in the detector.

Background-free searches for single or few-electron events are experimentally challenging. Sensitivity to such events has been demonstrated using two-phase time projection chambers with noble liquid targets, using data from XENON10 [6–8], XENON100 [7, 9], and DarkSide-50 [10]. Significant progress can be made by utilizing solid-state detectors, which exhibit much lower thresholds due to their typical low band gap. Recently, silicon Charge-Coupled Devices (CCDs) with a special "Skipper" readout stage [11] and high-voltage cryogenic silicon detectors with transition edge sensor readout [12] have demonstrated single-electron sensitivity. The 1.1 eV band gap of silicon allows for a DM mass threshold that is an order of magnitude lower than that achieved in noble liquid detectors, and permits significantly larger DM-electron scattering rates [5, 7, 13–15].

The Sub-Electron-Noise Skipper CCD Experimental Instrument (SENSEI) is designed to utilize the Skipper-CCD technology demonstrated in [11] to search for electron recoils from sub-GeV DM [16]. While the ultimate goal of the SENSEI Collaboration is to build a 100-gram detector consisting of multiple Skipper-CCDs, a prototype detector is currently operating ∼100 m underground near the MINOS experiment at Fermi National Accelerator Laboratory (FNAL). This prototype was first tested on the surface, collecting 0.019-gram-days of data (before analysis cuts).

In this letter, we present the first constraints on sub-GeV DM derived from SENSEI commissioning data. We exclude novel parameter space for DM masses below ∼4 MeV, above which the XENON10 constraint from [6, 7] dominates. Furthermore, operating on the surface allows a search for DM that strongly interacts with the visible sector. Such DM does not penetrate the Earth, and detectors placed deep underground, such

This document was prepared by [SENSEI Collaboration] using the resources of the Fermi National Accelerator Laboratory (Fermilab), a U.S. Department of Energy, Office of Science, HEP User Facility. Fermilab is managed by Fermi Research Alliance, LLC (FRA), acting under Contract No. DE-AC02-07CH11359

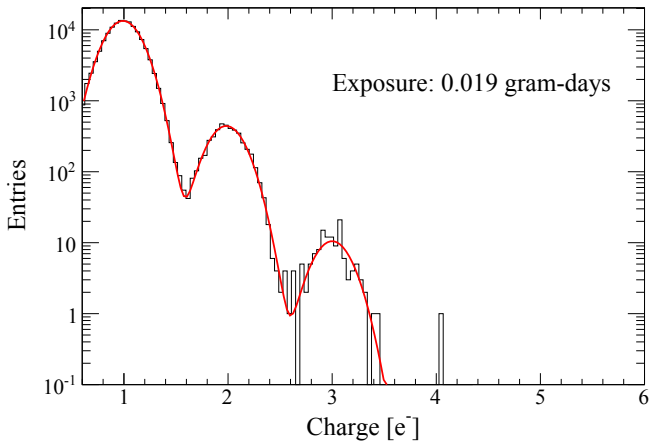

FIG. 1. Recorded spectrum after selection cuts for the 0.019 gram-days of commissioning data. Gaussian fits to the peaks show there are 140,302, 4676, 131, and 1 event(s) with 1, 2, 3, and 4 electrons, respectively. No events are seen for 5 − 100 electrons. The gaussian width of the peaks are $\sim 0.14 e^-$.

as the noble-liquid detectors mentioned above, have no sensitivity. Despite large cosmic-ray backgrounds, this region can be easily probed by a detector on the surface with a small amount of data. The SENSEI data thus also place novel constraints on DM particles with masses of several hundred MeV.

THE SENSEI PROTOTYPE DETECTOR

We use a single Skipper-CCD with an initial active mass of 0.094 grams of silicon fabricated parasitically in a production run for astronomical CCDs. The CCD has 724×1248 pixels of size $15\mu\text{m} \times 15\mu\text{m}$ and a thickness of 200μm. The Skipper-CCD was packaged in a light-tight copper housing that was cooled to an estimated 130 K to reduce the dark current on the sensor and to reduce the emission of infrared photons from black-body radiation. The sensor was read by a modified Monsoon electronics system described in [11].

This detector was used to take a small amount of commissioning data on May 11, 2017, at the Silicon Detector Facility (SiDet) at FNAL. SiDet has an elevation of $\sim$220 m above sea level and a roof consisting of about 7.6 cm of concrete, 2 mm of aluminum, and 1 cm of wood. The thickness of the light-tight copper housing in which the sensor was placed is 3 mm. The Skipper-CCD was read continuously for 427 minutes producing 18 images with 200 rows each. The single-sample noise of the CCD varied slightly from quadrant to quadrant. One of the quadrants had unusually high noise due to a charge transfer inefficiency problem in the readout stage, and all data from it were immediately discarded, leaving an active mass of 0.071 grams. The other three had a single-sample readout noise of $\sim 4\,\text{e}^-$; 800 samples were taken for each pixel, reducing the noise to $\sim 0.14\,\text{e}^-$.

Cuts \ $N_{e,\text{min}}$	1	2	3	4	5
1. Single pixel	1	0.62	0.48	0.41	0.37
2. Nearest Neighbor	0.8	0.8	0.8	0.8	0.8
3. Noise	0.88	0.88	0.88	0.88	0.88
4. Bleeding	0.95	0.95	0.95	0.95	0.95
Total	0.67	0.41	0.32	0.27	0.24
Number of events	140,302	4,676	131	1	0

TABLE I. Efficiencies for the data selection cuts for events with 1 to 5 electrons. The bottom row lists the number of observed events after cuts.

DATA SELECTION

The prototype Skipper-CCD has a dark current that was measured to be $\sim 1.14\,\text{e}^-$/pixel/day (this is orders of magnitude higher than is expected from the Skipper-CCDs that will be used by SENSEI in the future, which are produced in a dedicated production run using high-resistivity silicon). This leads to a large number of 1-, 2-, and 3-electron events. In this paper, we do not attempt to analyze the dark current in detail or to remove any background events. Instead, we place conservative limits by assuming that all events are from DM.

After data collection, we implemented several standard quality cuts for CCD-based detectors [18, 19] as well as cuts specific to our analysis:

- **Single pixel**. A DM event consists of one or more electrons that are created initially in a single pixel and spread with uniform probability along the height of the pixel. However, the electrons can drift apart as they diffuse to the surface, allowing some electrons to diffuse to a neighboring pixel. To simplify our analysis, we require the DM signal to fall within a single pixel. This cut also rejects neighboring dark-current coincidences.
- **Nearest Neighbor**. A DM event can fall adjacent to another signal or background event. Due to the single-pixel cut above and the poor timing resolution, we must remove the four nearest neighbors from all pixels that contain one or more electrons.
- **Noise**. We veto images in which the readout noise is 30% larger than the expected readout noise as inferred from an over-scan region in which virtual (non-existent) pixels are read.
- **Bleeding**. At low temperatures the electron mobility may be impeded, implying a small probability that an electron can get stuck in a given pixel for several downward shifts. If an event, such as a cosmic ray, produces a large number of electrons in some pixel(s), then pixels with several electrons may be found upstream in

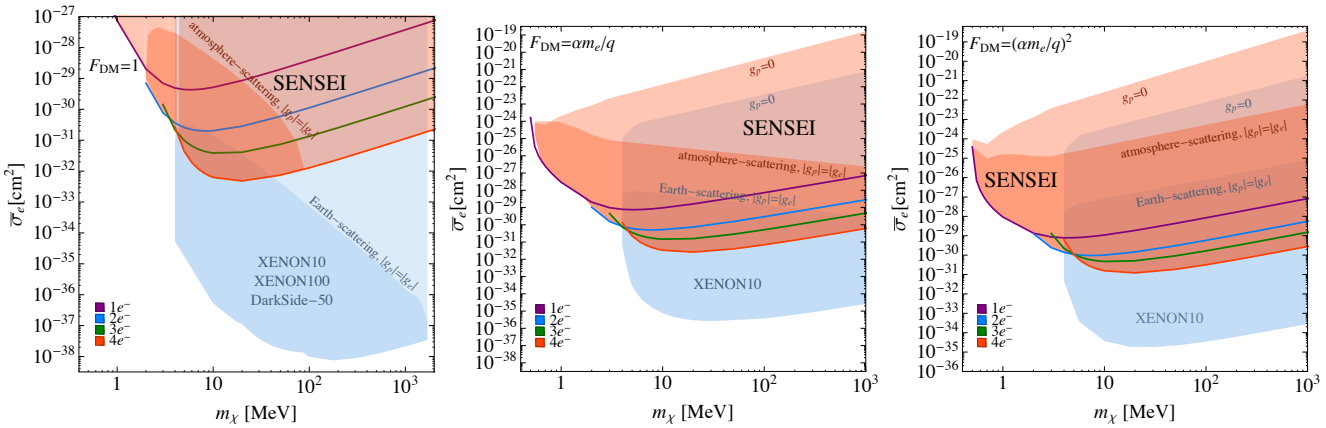

FIG. 2. The 95% C.L. constraints on the DM-electron scattering cross-sections, $\overline{\sigma}_e$, as a function of DM mass, m_χ, from a commissioning run above ground at FNAL using the SENSEI prototype detector. We show different DM form factors, $F_{\rm DM}(q) = 1$, $\alpha m_e/q$, and $(\alpha m_e/q)^2$. The purple, blue, green, and red lines correspond to the strongest constraints, from using events with exactly 1, 2, 3, or 4 electrons, respectively. The blue shaded regions are the current constraints from DM-electron scattering from XENON10, XENON100, and DarkSide-50. For large cross sections, the DM is stopped in the Earth's crust (atmosphere) and does not reach the noble-liquid (SENSEI prototype) detectors: the dark-shaded regions (labelled $|g_p| = |g_e|$) show preliminary results from [17] and are the excluded parameter regions assuming the interaction between DM and ordinary matter is mediated by a heavy dark photon (left), an electric dipole moment (middle), or an ultralight dark photon (right). The light-shaded regions (labelled $g_p = 0$) are the approximate excluded parameter regions assuming a mediator that couples only to electrons. The terrestrial effects shown here are order-of-magnitude estimates only, and more detailed calculations will appear in [17].

the image. We mask 10 pixels upstream of any pixel containing more than 100 electrons.

In what follows we bin the data, after the above selection cuts, according to the number of electrons per pixel, and derive constraints for each bin separately. Table I lists the selection efficiencies for electron bins $1-5$, calculated in a data-driven manner. The spectrum after cuts is shown in Fig. 1, together with gaussian fits to the first three bins. We use the bins with $1-100$ electrons in our analysis.

ANALYSIS AND RESULTS

We calculate the DM recoil spectrum for several models, deriving constraints both on DM-electron scattering and on bosonic DM being absorbed by an electron [20–23]. For the scattering case, we use the calculations and conventions from [5, 13]. We present our results in the $\overline{\sigma}_e$ versus m_χ parameter space for various DM form-factors, $F_{\rm DM}(q)$, where m_χ is the DM mass and $\overline{\sigma}_e$ is the cross section for DM to scatter off a free electron with the momentum transfer fixed to its typical value, $q = \alpha m_e$, where α is the fine-structure constant and m_e is the electron mass. $F_{\rm DM}(q)$ parameterizes the model-dependent momentum dependence of the DM interaction: a "heavy" mediator with mass $\gg \alpha m_e$ has $F_{\rm DM}(q) = 1$; an "ultralight" mediator with mass $\ll \alpha m_e$ has $F_{\rm DM}(q) = (\alpha m_e/q)^2$; and an electric-dipole-moment interaction with the Standard-Model photon produces $F_{\rm DM}(q) \simeq \alpha m_e/q$.

For bosonic DM, we will consider that the DM is a dark photon, denoted A', with mass $m_{A'}$, that is stable on the lifetime of the Universe. We follow the calculations and conventions in [21], and present results in the ϵ versus $m_{A'}$ parameter space, where ϵ is the parameter that characterizes the strength of the kinetic mixing between the A' and the photon.

For each model, we calculate conservative 95% confidence level upper limits using Poisson statistics and assuming that all observed electrons in a given bin are DM events. We compare the resulting limit from each bin with the predicted number of DM events (for a given value of $\overline{\sigma}_e$ or ϵ), after correcting for the efficiencies.

Our main results, for $\overline{\sigma}_e$ versus m_χ are shown in Fig. 2 for the three form factors discussed above. The black line denotes the overall SENSEI limit, while the colored lines show the limits from each bin separately. The 1-, 2-, and 4-electron bins essentially set the strongest constraints in different parts of the mass range.

Despite a small exposure time on the surface, the SENSEI commissioning run already probes novel parameter space for light DM (mass $\lesssim 4$ MeV) and for DM with large cross sections. This is the first time that a direct-detection constraint is derived for DM masses as low as $\sim$500 keV. In contrast, noble-liquid experiments (especially XENON10) probe lower cross sections for masses $\gtrsim 4$ MeV.

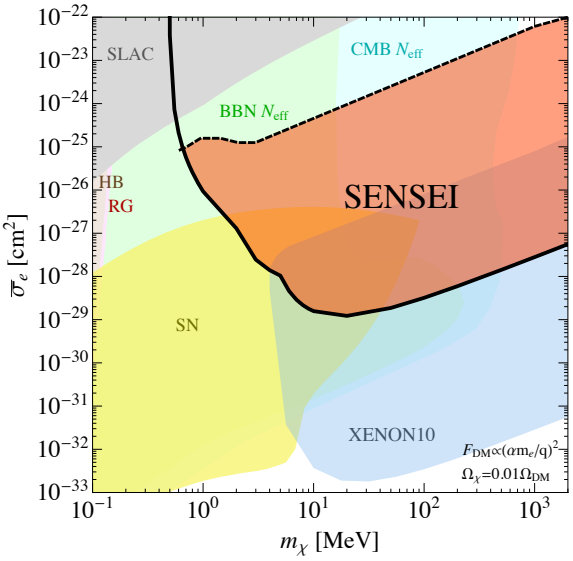

FIG. 3. The 95% C.L. constraint on $\overline{\sigma}_e$ versus m_χ for $F_{\rm DM}(q^2) = (\alpha m_e/q)^2$ from a surface run at FNAL using the SENSEI prototype detector (red region, bounded below by a solid line and above by a dashed line that is the same as the $|g_p| = |g_e|$ line in the right plot of Fig. 2 [17]). We assume that χ couples to an ultralight dark-photon mediator, and $\Omega_\chi = 0.01\Omega_{\rm DM}$, which may explain the 21-cm signal observed by EDGES. Other constraints are described in the text. The SENSEI surface run disfavors a small region of previously open parameter space for $\overline{\sigma}_e \gtrsim 10^{-25}$ cm^2 and m_χ greater than a few hundred MeV.

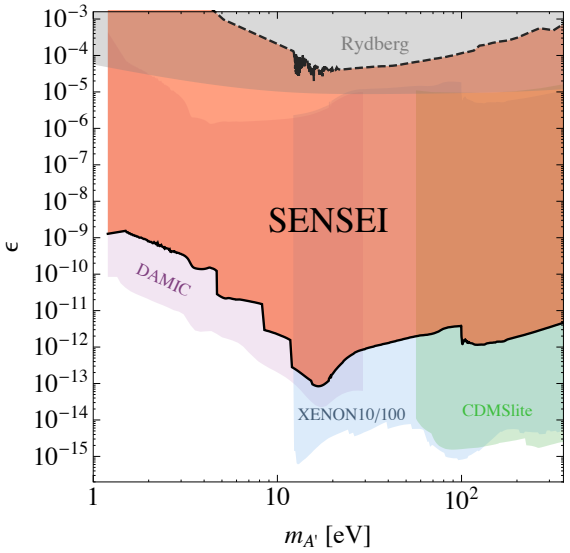

FIG. 4. Constraints on dark-photon DM absorption by electrons, in the kinetic mixing (ϵ) versus dark-photon mass ($m_{A'}$) parameter space from a surface run at FNAL using the SENSEI prototype detector (red). Constraints from XENON10, XENON100, CDMSlite, DAMIC, and a measurement of the Rydberg constant are also shown. The direct-detection constraints are absent at large ϵ, where the A' is absorbed in the Earth's crust or atmosphere before reaching the detector. The SENSEI constraint closes a gap in laboratory probes of the high-ϵ region. See text for details.

Second, the noble-liquid detectors that have previously constrained sub-GeV DM are operated underneath the Gran Sasso mountain. DM that interacts strongly with ordinary matter cannot reach these detectors due to scattering in the Earth. In contrast, much larger interaction strengths can be probed with the SENSEI surface run, since only the atmosphere (and a thin roof) can stop the DM.

The terrestrial effects on MeV-to-GeV DM scattering off nuclei or electrons are model-dependent and have so far only been explored partially in the literature [24, 25]; a full exploration is beyond the scope of this paper (see [26–31] for larger DM masses). However, to illustrate that SENSEI constrains novel parameter space at large cross sections, we include very preliminary results from [17]. If the interaction between DM and ordinary matter is mediated by a dark photon or an electric-dipole-moment, the DM will dominantly scatter off *nuclei* in the atmosphere or Earth before reaching the detector, where it scatters off an *electron* to leave an observable signal. The darker shaded regions in Fig. 2 (labelled "$|g_p| = |g_e|$") illustrate the cross sections above which the respective detectors have no sensitivity, assuming the DM interaction with ordinary matter is mediated by a heavy dark photon, an electric dipole moment, or an ultralight dark photon in the left, middle, and right plots, respectively. If the mediator only couples to electrons (and not to nuclei), a very naive rescaling of the preliminary results in [17] leads to the excluded regions labelled "$g_p = 0$" (lighter shaded regions). We see that the SENSEI prototype constraints are largely complementary to existing noble-liquid detector constraints.

We give one example of a concrete model that can give rise to large cross sections in Fig. 3. We assume that a subdominant DM component, χ, interacts with an ultralight dark photon ($m_{A'} \ll$ keV), with $\Omega_\chi = 0.01\Omega_{\rm DM}$. This model is motivated by the EDGES measurement of the 21-cm spectrum at $z \simeq 17$, which revealed an anomalously large absorption signal [32] [33] (see also [34–49]). The SENSEI constraint (red) is bounded by the solid (dashed) line for small (large [17]) $\overline{\sigma}_e$. It disfavors novel parameter space for DM masses above a few hundred MeV for $\overline{\sigma}_e \gtrsim 10^{-25}$ cm^2, which is the preliminary value of the upper boundary of the XENON10 constraint [17]. Other constraints arise from the SLAC millicharge experiment [50], red-giant (RG) and horizontal-branch (HB) stars [51], the BBN and CMB measurements of the number of relativistic degrees of freedom ($N_{\rm eff}$) [51], and Supernova 1987A (SN) [52]. A more careful analysis of other possible constraints in this re-

gion is, however, warranted, including a re-analysis of low-threshold DM-nuclear recoil data [2, 3], and an analysis of whether such a DM candidate would be evacuated from the Galactic disk by Galactic magnetic fields and supernova shock waves (as may be the case if the DM has a millicharge [53]).

We next present the SENSEI prototype constraints on ϵ versus $m_{A'}$ for dark-photon DM (A'), which can be absorbed by an electron, in Fig. 4. At small ϵ, the SENSEI prototype constraint is weaker than other constraints due to its small exposure, however, for large ϵ new grounds are explored. We estimate the maximal coupling, $\epsilon_{\rm max} = 1/\sqrt{\rho L \sigma_{\rm abs}}$ above which the A' is absorbed by molecules in the atmosphere or by atomic electrons in the Earth's crust and sensitivity is lost. Here $\sigma_{\rm abs}$ is the measured photoabsorption cross-sections per molecule, N is the average density, and L is the depth. For simplicity, we take the Earth's crust to consist of silicon with $\rho = 2.7$ g/cm^3, with $L = 0.7$ km (CDMSlite), 1.4 km (XENON10/100), or 2 km (DAMIC). We take the atmosphere to consist of O_2 and N_2 [54] (with $\rho = 1.2 \times 10^{-4}$ g/cm^3 and $L = 86$ km). These dominate the absorption for $m_{A'} \gtrsim 5$ eV, the bond-dissociation energy of O_2 (no data on $\sigma_{\rm abs}$ is available below $m_{A'} \simeq 10$ eV, so we extrapolate the available data down to 5 eV). For $m_{A'} \lesssim 5$ eV, ozone dominates the absorption, but its abundance is very small and does not affect the region shown in Fig. 4. We see that SENSEI closes a gap in laboratory probes of the large-ϵ region: the gap was bounded above by a measurement of the Rydberg constant (we show a 2σ constraint adapted from [55–57]) and below by our analysis of terrestrial absorption effects for XENON10, XENON100, CDMSlite, and DAMIC [4, 20–22, 58] Note that stellar constraints [59, 60] may already disfavor this region; however, a more careful analysis of these bounds at high-ϵ is warranted.

SUMMARY AND OUTLOOK

We present results from a low-exposure commissioning run of a SENSEI prototype detector. We demonstrate the first use of Skipper-CCD technology for a DM search, the first direct-detection constraints for DM masses $0.5 - 4$ MeV, and the first direct-detection constraints on strongly interacting DM for masses between 0.5 MeV and a few hundred MeV. Over the next few years, the SENSEI Collaboration aims to construct a detector consisting of ∼100 grams of Skipper CCDs that are fabricated in a dedicated production run using high-resistivity silicon. These detectors are expected to have a dark current several orders of magnitude lower than the prototype detector and an improved single-sample noise. We expect to collect an exposure that is almost 2 million times larger than the exposure of the surface run and with far fewer background events, allowing us to explore vast new regions of DM parameter space.

ACKNOWLEDGMENTS

We are grateful to Timon Emken, Chris Kouvaris, and Mukul Sholapurkar for extensive discussions and for letting us include very preliminary results from the upcoming paper [17]. We also thank Alex Drlica-Wagner for carefully reading a draft of the paper and for numerous useful comments. We are grateful for the support of the Heising-Simons Foundation under Grant No. 79921. RE also acknowledges support from DoE Grant desc0017938. This work was supported by Fermilab under DOE Contract No. DE-AC02-07CH11359. The work of TV is supported by the I-CORE Program of the Planning Budgeting Committee and the Israel Science Foundation (grant No.1937/12), by the European Research Council (ERC) under the EU Horizon 2020 Programme (ERC-CoG-2015 - Proposal n. 682676 LDMThExp), by the Israel Science Foundation-NSFC (grant No. 2522/17) and by the German-Israeli Foundation (grant No. I-1283-303.7/2014). TV is further supported by a grant from The Ambrose Monell Foundation, given by the Institute for Advanced Study. RE and TV are also funded by the Binational Science Foundation (grant No. 2016153).

* mike@fnal.gov
† rouven.essig@stonybrook.edu
‡ estrada@fnal.gov
§ fmoroni.guillermo@gmail.com
¶ javiert@fnal.gov
** miguelsofoharo@gmail.com
†† tomerv@post.tau.ac.il
‡‡ tien-tien.yu@cern.ch

[1] M. Battaglieri *et al.*, (2017), arXiv:1707.04591 [hep-ph].
[2] G. Angloher *et al.* (CRESST), Eur. Phys. J. **C77**, 637 (2017), arXiv:1707.06749 [astro-ph.CO].
[3] F. Petricca *et al.* (CRESST), in *15th International Conference on Topics in Astroparticle and Underground Physics (TAUP 2017) Sudbury, Ontario, Canada, July 24-28, 2017* (2017) arXiv:1711.07692 [astro-ph.CO].
[4] R. Agnese *et al.* (SuperCDMS), Phys. Rev. Lett. **116**, 071301 (2016), arXiv:1509.02448 [astro-ph.CO].
[5] R. Essig, J. Mardon, and T. Volansky, Phys. Rev. **D85**, 076007 (2012), arXiv:1108.5383 [hep-ph].
[6] R. Essig, A. Manalaysay, J. Mardon, P. Sorensen, and T. Volansky, Phys. Rev. Lett. **109**, 021301 (2012), arXiv:1206.2644 [astro-ph.CO].
[7] R. Essig, T. Volansky, and T.-T. Yu, Phys. Rev. **D96**, 043017 (2017), arXiv:1703.00910 [hep-ph].
[8] J. Angle *et al.* (XENON10), Phys. Rev. Lett. **107**, 051301 (2011), [Erratum: Phys. Rev. Lett.110,249901(2013)], arXiv:1104.3088 [astro-ph.CO].
[9] E. Aprile *et al.* (XENON100), (2016), arXiv:1605.06262 [astro-ph.CO].

[10] P. Agnes *et al.* (DarkSide), (2018), arXiv:1802.06998 [astro-ph.CO].

[11] J. Tiffenberg, M. Sofo-Haro, A. Drlica-Wagner, R. Essig, Y. Guardincerri, S. Holland, T. Volansky, and T.-T. Yu, Phys. Rev. Lett. **119**, 131802 (2017), arXiv:1706.00028 [physics.ins-det].

[12] R. K. Romani *et al.*, (2017), arXiv:1710.09335 [physics.ins-det].

[13] R. Essig, M. Fernandez-Serra, J. Mardon, A. Soto, T. Volansky, and T.-T. Yu, JHEP **05**, 046 (2016), arXiv:1509.01598 [hep-ph].

[14] S. K. Lee, M. Lisanti, S. Mishra-Sharma, and B. R. Safdi, Phys. Rev. **D92**, 083517 (2015), arXiv:1508.07361 [hep-ph].

[15] P. W. Graham, D. E. Kaplan, S. Rajendran, and M. T. Walters, Phys.Dark Univ. **1**, 32 (2012), arXiv:1203.2531 [hep-ph].

[16] T. S. Collaboration, to appear.

[17] T. Emken, R. Essig, C. Kouvaris, and M. Sholapurkar, to appear.

[18] A. Aguilar-Arevalo *et al.* (CONNIE), *Proceedings, 15th Mexican Workshop on Particles and Fields (MWPF 2015): Mazatlán, México, November 2-6, 2015*, J. Phys. Conf. Ser. **761**, 012057 (2016), arXiv:1608.01565 [physics.ins-det].

[19] A. Aguilar-Arevalo *et al.* (DAMIC), Phys. Rev. **D94**, 082006 (2016), arXiv:1607.07410 [astro-ph.CO].

[20] H. An, M. Pospelov, J. Pradler, and A. Ritz, Phys. Lett. **B747**, 331 (2015), arXiv:1412.8378 [hep-ph].

[21] I. M. Bloch, R. Essig, K. Tobioka, T. Volansky, and T.-T. Yu, JHEP **06**, 087 (2017), arXiv:1608.02123 [hep-ph].

[22] Y. Hochberg, T. Lin, and K. M. Zurek, (2016), arXiv:1608.01994 [hep-ph].

[23] Y. Hochberg, T. Lin, and K. M. Zurek, Phys. Rev. **D94**, 015019 (2016), arXiv:1604.06800 [hep-ph].

[24] T. Emken, C. Kouvaris, and I. M. Shoemaker, Phys. Rev. **D96**, 015018 (2017), arXiv:1702.07750 [hep-ph].

[25] T. Emken and C. Kouvaris, JCAP **1710**, 031 (2017), arXiv:1706.02249 [hep-ph].

[26] G. D. Mack, J. F. Beacom, and G. Bertone, Phys. Rev. **D76**, 043523 (2007), arXiv:0705.4298 [astro-ph].

[27] B. J. Kavanagh, R. Catena, and C. Kouvaris, JCAP **1701**, 012 (2017), arXiv:1611.05453 [hep-ph].

[28] J. H. Davis, Phys. Rev. Lett. **119**, 211302 (2017), arXiv:1708.01484 [hep-ph].

[29] M. S. Mahdawi and G. R. Farrar, JCAP **1712**, 004 (2017), arXiv:1709.00430 [hep-ph].

[30] M. S. Mahdawi and G. R. Farrar, (2017), arXiv:1712.01170 [hep-ph].

[31] D. Hooper and S. D. McDermott, (2018), arXiv:1802.03025 [hep-ph].

[32] J. D. Bowman, A. E. E. Rogers, R. A. Monsalve, T. J. Mozdzen, and N. Mahesh, Nature **555**, 67 (2018).

[33] R. Barkana, N. J. Outmezguine, D. Redigolo, and T. Volansky, (2018), arXiv:1803.03091 [hep-ph].

[34] H. Tashiro, K. Kadota, and J. Silk, Phys. Rev. **D90**, 083522 (2014), arXiv:1408.2571 [astro-ph.CO].

[35] J. B. Muñoz, E. D. Kovetz, and Y. Ali-Haïmoud, Phys. Rev. **D92**, 083528 (2015), arXiv:1509.00029 [astro-ph.CO].

[36] R. Barkana, Nature **555**, 71 (2018), arXiv:1803.06698 [astro-ph.CO].

[37] J. B. Muñoz and A. Loeb, (2018), arXiv:1802.10094 [astro-ph.CO].

[38] A. Berlin, D. Hooper, G. Krnjaic, and S. D. McDermott, (2018), arXiv:1803.02804 [hep-ph].

[39] S. Fraser *et al.*, (2018), arXiv:1803.03245 [hep-ph].

[40] G. D'Amico, P. Panci, and A. Strumia, (2018), arXiv:1803.03629 [astro-ph.CO].

[41] Z. Kang, (2018), arXiv:1803.04928 [hep-ph].

[42] Y. Yang, X. Huang, and L. Feng, (2018), arXiv:1803.05803 [astro-ph.CO].

[43] M. Pospelov, J. Pradler, J. T. Ruderman, and A. Urbano, (2018), arXiv:1803.07048 [hep-ph].

[44] M. Safarzadeh, E. Scannapieco, and A. Babul, (2018), arXiv:1803.08039 [astro-ph.CO].

[45] S. Clark, B. Dutta, Y. Gao, Y.-Z. Ma, and L. E. Strigari, (2018), arXiv:1803.09390 [astro-ph.HE].

[46] K. Cheung, J.-L. Kuo, K.-W. Ng, and Y.-L. S. Tsai, (2018), arXiv:1803.09398 [astro-ph.CO].

[47] T. R. Slatyer and C.-L. Wu, (2018), arXiv:1803.09734 [astro-ph.CO].

[48] H. Liu and T. R. Slatyer, (2018), arXiv:1803.09739 [astro-ph.CO].

[49] A. Falkowski and K. Petraki, (2018), arXiv:1803.10096 [hep-ph].

[50] A. A. Prinz *et al.*, Phys. Rev. Lett. **81**, 1175 (1998), arXiv:hep-ex/9804008 [hep-ex].

[51] H. Vogel and J. Redondo, JCAP **1402**, 029 (2014), arXiv:1311.2600 [hep-ph].

[52] J. H. Chang, R. Essig, and S. D. McDermott, (2018), arXiv:1803.00993 [hep-ph].

[53] S. D. McDermott, H.-B. Yu, and K. M. Zurek, Phys. Rev. **D83**, 063509 (2011), arXiv:1011.2907 [hep-ph].

[54] J. Fennelly and D. Torr, Atomic Data and Nuclear Data Tables **51**, 321 (1992).

[55] V. Popov, Turkish Journal of Physics **23**, 943 (1999).

[56] S. G. Karshenboim, Phys. Rev. **D82**, 073003 (2010), arXiv:1005.4872 [hep-ph].

[57] S. G. Karshenboim, Phys. Rev. Lett. **104**, 220406 (2010), arXiv:1005.4859 [hep-ph].

[58] A. Aguilar-Arevalo *et al.* (DAMIC), Phys. Rev. Lett. **118**, 141803 (2017), arXiv:1611.03066 [astro-ph.CO].

[59] H. An, M. Pospelov, and J. Pradler, Phys. Lett. **B725**, 190 (2013), arXiv:1302.3884 [hep-ph].

[60] J. Redondo and G. Raffelt, JCAP **1308**, 034 (2013), arXiv:1305.2920 [hep-ph].